LEGIBILITY NOTICE

A major purpose of the Technical Information Center is to provide the broadest dissemination possible of information contained in DOE's Research and Development Reports to business, industry, the academic community, and federal, state and local governments.

Although a small portion of this report is not reproducible, it is being made available to expedite the availability of information on the research discussed herein.

CONF-8710806--2

Los Alamos National Laboratory is operated by the University of California for the United States Department of Energy under contract W-7405-ENG-36

TITLE APPLICATIONS OF A THEORY OF FERROMAGNETIC HYSTERESIS

LA-UR--87-2722

DE87 014725

AUTHOR(S) M. L. Hodgdon, M-6

SUBMITTED TO COMPUMAG CONF.,
Graz, Austria
Aug. 24-28, 1987

DISCLAIMER

Los Alamos Los Alamos National Laboratory
Los Alamos, New Mexico 87545

FORM NO. 836 R4
ST. NO. 2629 5/81

MASTER

APPLICATIONS OF A THEORY OF FERROMAGNETIC HYSTERESIS

Marion L. Hodgdon
Los Alamos National Laboratory
Los Alamos, New Mexico 87545

ABSTRACT

The differential equation $\dot{B} = \alpha|\dot{H}|[f(H) - B] + \dot{H}g(H)$ and a set of restrictions on the material functions f and g yield a theory of rate independent hysteresis for isoperm ferromagnetic materials. A modification based on exchanging the positions of B and H in the differential equation and on allowing for the dependence of the material functions on $\dot{H}$ extends the theory to rate dependent, nonisoperm materials. The theory and its extension exhibit all of the important features of ferromagnetic hysteresis, including the existence and stability of minor loops. Both are well suited for use in numerical field solving codes. Examples in which the material functions are simple combinations of analytic functions are presented here for Mn-Zn ferrite, Permalloy, CMD5005, and CoCr thin film. Also presented is a procedure for constructing a two dimensional vector model that yields bell-shaped and M-shaped curves for graphs of the angular variation of the coercive field.

INTRODUCTION

Work by Coleman and Hodgdon [1,2] and by Bouc [3] shows that the differential equation,

$$\dot{B} = \alpha|\dot{H}|[f(H) - B] + \dot{H}g(H), \qquad (1)$$

relating the time rate of change of the flux density B to that of the magnetic field H, along with a set of constraints on α and on the material functions f and g, yields a theory that is in agreement with the essential features of one dimensional, rate independent ferromagnetic hysteresis. These include the existence of a major loop that encloses all of the states (H, B) accessible from the demagnetized state, the existence of stable minor loops, the convergence of solution curves to the appropriate minor loop for fields that oscillate between two extreme points, nonnegative values for the energy expended in the traversal of a minor loop, and agreement in sign between $\dot{B}$ and $\dot{H}$. In this theory, the functions f and g must meet the following restrictions:

i) f must be a piecewise smooth, monotone increasing, odd function of H, with a derivative, f', that obtains a finite limit $f'(\infty)$ for large H;

ii) g must be a piecewise continuous, even function of H, with a finite limit satisfying $g(\infty) = f'(\infty)$; and

iii) for all finite H, the functions f' and g must satisfy the inequalities

$$f'(H) \geq g(H) \geq \alpha e^{\alpha H} \int_H^\infty [f'(\varsigma) - g(\varsigma)] e^{-\alpha \varsigma} d\varsigma.$$

As shown in [1] and [2], (1) can be written as the set of equations

$$\frac{dB}{dH} = \begin{cases} \alpha[f(H) - B] + g(H), & \text{for } \dot{H} > 0; \\ -\alpha[f(H) - B] + g(H), & \text{for } \dot{H} < 0, \end{cases} \tag{2}$$

for the slopes of hysteresis curves in the H-B plane. These equations are convenient forms of (1) for both numerical and analytic work. When $\dot{H} > 0$, the solutions $B(H)$ obtained by integration of (2a) give the ascending portions of hysteresis loops; when $\dot{H} < 0$, the solutions $B(H)$ of (2b) are the descending portions.

Functions f and g have been found that satisfy *i*–*iii* and yield solution curves of (2) that are in good agreement with those of ferromagnetically soft, isoperm materials, such as the Mn-Zn ferrite shown in Fig. 1.

By interchanging the positions of H and B in (1) and revising the restrictions on the material functions, the theory can be extended to include square loop materials. Under these modifications, the differential equation is

$$\dot{H} = \alpha |\dot{B}| [\tilde{f}(B) - H] + \dot{B} \tilde{g}(B), \tag{3}$$

or, in terms of the local magnetic permeability,

$$\frac{dB}{dH} = \begin{cases} [\alpha[\tilde{f}(B) - H] + \tilde{g}(B)]^{-1}, & \text{for } \dot{H} > 0, \\ [-\alpha[\tilde{f}(B) - H] + \tilde{g}(B)]^{-1}, & \text{for } \dot{H} < 0. \end{cases} \tag{4}$$

The restrictions on $\tilde{f}$, $\tilde{g}$, and α are that

iv) $\tilde{f}$ be a piecewise smooth, odd function of B, with a derivative $\tilde{f}'$ which obtains the finite limit $\tilde{f}'(\infty)$;

v) $\tilde{g}$, a piecewise continuous, even function of B, with the limit $\tilde{g}(\infty) = \tilde{f}'(\infty)$; and

vi) for all B, $\tilde{g}$ must satisfy the inequality

$$\tilde{g}(B) \geq \max\left\{\tilde{f}'(B),\ \alpha e^{\alpha B}\left|\int_B^\infty [\tilde{f}'(\zeta) - \tilde{g}(\zeta)]e^{-\alpha\zeta}\,d\zeta\right|\right\}.$$

The development of the restrictions and their implications for the solutions of (1) are discussed in [1] and [2]. In this paper, I will demonstrate the application of the theory, in the form of eqs. (3) and (4), to a variety of materials and to two problems, one involving rate dependence and the other, the anisotropy exhibited by thin films used in magnetic recording.

SOLUTIONS AND APPLICATIONS

Representation of experimentally determined hysteresis loops by the solutions of (3) and (4) requires a value† for α, and functional forms and values for $\tilde{f}$ and $\tilde{g}$. When $\tilde{f}$ and $\tilde{g}$ are piecewise linear functions with only two pieces, closed form solutions of (3) can be obtained [1]. These solutions are useful in that they require only function evaluation, rather than numerical integration. Solutions for cases in which other material functions are used must be obtained by numerical integration. For the functions described below, the simple finite difference form of (4)

$$B(i+1) \quad B(i) + [+\alpha|\hat{f}(B_i) \quad H_i| + \tilde{g}(B_i)]^{-1}(H_{i+1} - H_i), \quad (5)$$

along with a specification of an initial state (H_0, B_0), the initial sign of $\dot{H}$, and a list of the turning points of H, appears sufficient.‡ The curves shown in Figs. 2, 4-5, and 7-9 were computed in this way.

† α 1 in all examples in this paper.

‡ Although either B or H may be taken as the independent variable in (3), solutions are presented here for cases in which H and $\dot{H}$ are given and solution curves $B(H)$ are required.

Selection and construction of the material functions can be guided by the results given in [1] and [2] that

a)the graph of the function $\tilde{f}$ is the inverse of the anhysteretic or ideal magnetization curve [4], which lies, at each H, approximately half way between the ascending and descending portions of the major loop; and

b) on intervals where $\tilde{g}(B) = \tilde{f}'(B)$, the ascending and descending portions of the hysteresis loops coincide so that the loops degenerate into a single curve, as they do, for example, past the point where the major loop closes.

I have found the following forms for $\tilde{f}$ and $\tilde{g}$ useful in that they scale well for a variety of materials and that the values of the constants in them can be determined from available hysteresis data. They are simple, however, and yield approximations to measured hysteresis curves. In cases where accuracy greater than that shown here is required, the theory is agreeable to more complicated functions, such as piecewise linear ones with many sections taken from a sequence of measured points, and more complicated differencing schemes than (5). In this paper, all solutions are obtained with

$$\tilde{f}(B) = \begin{cases} A_1 \tan A_2 B, & \text{for } |B| \le B_{cl}; \\ A_1 \tan A_2 B_{cl} + (B - B_{cl})/\mu_{cl}, & \text{for } B > B_{cl}; \\ -A_1 \tan A_2 B_{cl} + (B + B_{cl})/\mu_{cl}, & \text{for } B < -B_{cl}; \end{cases} \tag{6a}$$

and

$$\tilde{g}(B) = \begin{cases} \tilde{f}'(B)\left[1 + A_3 \exp\left(\dfrac{A_4|B|}{B_{cl}|B|}\right)\right], & \text{for } |B| \le B_{cl}; \\ \tilde{f}'(B), & \text{for } |B| > B_{cl}, \end{cases} \tag{6b}$$

where, as shown in Fig. 2, B_{cl} is the flux density at the point in the first quadrant of the H – B plane where the major loop closes and μ_{cl} is the slope beyond the closure point. The values for the material constants A_1 through A_4 can be obtained from the value of α, and from values of the flux density B_{cl}, the magnetic field H_{cl}, and the slope μ_a at the closure point of the major loop; the slope μ_{cl} beyond

the closure point; the value of the flux density B_r at full magnetic remanence, and the slope μ_r of the major loop at remanence; the coercive field H_c, and the slope μ_c of the major loop at the coercive point. A_2 is the solution of the equation

$$2H_{cl}\mu_s A_2 - \sin(2B_{cl}A_2) = 0. \tag{7a}$$

Values for A_1, A_3, and A_4 are calculated as follows:

$$A_1 = H_{cl}\cot(A_2 B_{cl}), \tag{7b}$$

$$A_3 = 1 - \frac{1}{A_1 A_2}\left[\frac{1}{\mu_c} - \alpha H_c\right], \tag{7c}$$

and

$$A_4 = \frac{B_r - B_{cl}}{B_r}\ln\left[\frac{1}{A_3} - \frac{\cos^2(\alpha B_r)}{A_1 A_2 A_3}\left(\frac{1}{\mu_r} + \alpha A_1 \tan(A_2 B_r)\right)\right]. \tag{7d}$$

The functions in (6) satisfy constraints *iv* and *v*. However, not all hysteresis data yield functions satisfying *vi*, and a numerical check is required. For most materials with loop shapes similar to those shown here, often only small adjustments in the slopes μ_c and μ_r bring $\tilde{f}$ and $\tilde{g}$ into agreement with *vi*. Values for the material constants for several materials are listed in Tables 1 and 2. For Permalloy, hysteresis curves and the functions $\tilde{f}$ and $\tilde{g}$ are shown in Figs. 2-4.

A RATE DEPENDENT PROBLEM

Of interest to transformer designers is the response of ferrites to pulses and sinusoidal variations of the applied field.† For fields which vary so slowly that there is virtually no lag between the field and the corresponding flux density, the rate independent theory in eqs. (3)-(6) is sufficient. Descriptions of rate dependent material behavior

† The resistivity of these ferrites is often so large that eddy currents and their effect on the lag between changes in flux density and applied field are negligible.

for rapidly varying fields are more complex and require ideas and expressions in addition to those in (3)-(6).

There are two catagories of rate dependent responses. One is the true pulse response in which the applied field changes instantaneously or almost instantaneously to a new value and then maintains that value while the material seeks an equilibrium. From earlier studies [5], magnetic materials subjected to such pulses obey rate laws through which the flux density $B(t)$ approaches an equilibrium value B_∞ as t becomes large. The material time constants lie between two extreme values τ_1 and τ_2, and $B(t)$ can be represented as the sum,

$$B(t) = \mu_0 H + \int_{\tau_1}^{\tau_2} b(t,\tau)d\tau. \tag{8}$$

For each τ between τ_1 and τ_2, the function b is the solution of the rate law

$$\frac{\partial b}{\partial t} = -\frac{1}{\tau}(b - b_\infty), \tag{9}$$

where the equilibrium value b_∞ is given by

$$b_\infty(\tau) = (B_\infty - \mu_0 H)[\tau \ln(\tau_2/\tau_1)]^{-1}. \tag{10}$$

In the studies given in [5], hysteresis is ignored, and B_∞ is assumed to be proportional to the pulse height H. A more complete description which includes hysteretic effects is obtained by using the rate independent theory in (3)-(6) to provide values for the equilibrium flux density B_∞ in eqs. (8)-(10). For instance, for a material initially in the state (H_0, B_0) subjected to a pulse of height H_1 that is maintained until the state (H_1, B_1) is reached and then released, the rate independent theory provides the equilibrium value, $B_\infty(H_1; H_0, B_0)$, associated with the previous state (H_0, B_0), and then the, possibly nonzero, remanent value, $B_\infty(0; H_1, B_1)$, associated with the state (H_1, B_1). Solutions of (8)-(10) provide the time course of the flux density as it varies from B_0 to B_1 and then toward remanence. Numerical implementation of this type of rate effect involves summations over the responses from previous pulses but is facilitated by

the result that the solutions of (8)-(10) can be written in terms of incomplete gamma functions, which are included on many standard numerical mathematics libraries.

In many practical situations, the second type of rate effect occurs in which neither the rate of change of the applied field nor that of the flux density are zero. The rise times of many pulses, for example, are slow enough that some, if not all of the material response occurs while the pulses are reaching their full height. Since sinusoidally varying applied fields also yield responses of this type, it is sometimes called an ac response. I have found a modification of (3) useful for these cases. The modified differential equation is

$$\dot{H} = \alpha|\dot{B}|[\tilde{f}(B) - H] + \dot{B}\hat{g}(B, \dot{H}). \tag{11}$$

As in the rate independent theory, $\tilde{f}$ must obey *iv*, and its graph coincides with the inverse of the anhysteretic curve. The function $\hat{g}$ must be an even function of B and of $\dot{H}$ with

$$\lim_{B\to\infty} \hat{g}(B, \dot{H}) = \tilde{f}'(\infty), \text{ and } \lim_{\dot{H}\to 0} \hat{g}(B, \dot{H}) = \tilde{g}(B);$$

$\tilde{g}$ is a function of B alone and satisfies *v* and *vi*. The limits imposed on $\hat{g}$ insure that, in agreement with experiments, the major loop closes, and hysteretic behavior, with the attributes of the rate independent model, is approached as the slow (or "dc") limit of the rate dependent one.

Physical significance and evaluation of $\hat{g}$ can be obtained for the simple form

$$\hat{g}(B, \dot{H}) = \tilde{g}(B)[1 + \bar{g}(B)c(\dot{H})], \tag{12}$$

where c is an even function of $\dot{H}$, $\bar{g}$ is an even function of B, and

$$\lim_{\dot{H}\to 0} c(\dot{H}) = 0, \text{ and } \lim_{B\to\infty} \bar{g}(B) = 0.$$

Substitution of (12) into (11) and division, where $\dot{B}$ does not change sign, by $\dot{B}$ yields an expression for the inverse of the magnetic permeability, which here depends on the instantaneous rate of change

of the magnetic field, $\dot{H}$, as well as on the state (H, B):

$$\frac{dH}{dB} = \pm\alpha[\tilde{f}(B) - H] + \tilde{g}(B) + \tilde{g}(B)\hat{g}(B)c(\dot{H}), \qquad (13)$$

By (4), $\pm\alpha[\tilde{f}(B) - H] + \tilde{g}(B)$ are permeabilities along rate independent curves. By the restrictions of $\hat{g}$, such curves are produced by slowly varying (or "dc") magnetic fields. Substitution of this result into (13) and rearrangement yields an expression for $\bar{g}(B)c(\dot{H})$ in terms of the difference between the inverses of the permeability at the point (H, B) along a curve corresponding to a slow, or in the limit, "dc" $(\dot{H} = 0)$ magnetic field, and the permeability or slope at the same point of a hysteresis curve corresponding to a more rapid variation in H:

$$\bar{g}(B)c(\dot{H}) = \frac{1}{\tilde{g}(B)}\left[\left(\frac{dH}{dB}\right)_{(H,B,\dot{H})} - \left(\frac{dH}{dB}\right)_{(H,B,0)}\right]. \qquad (14)$$

Here the triplet $(H, B, \dot{H})$ denotes the point (H, B) and the rate $\dot{H}$ at which the permeability is measured.

Graphs of the initial permeability μ_i *vs.* frequency ν are often supplied by experimenters along with dc hysteresis loops. In such cases, $\tilde{f}$ and $\tilde{g}$ of the rate independent theory may be evaluated using the dc data and functional forms such as those in (6). The combination $\bar{g}(0)c(\dot{H}(0))$, with $H(t) = H_M \sin(2\pi\nu t)$ and $\dot{H}(0) = 2\pi\nu H_M$, may be calculated from (13) as

$$\bar{g}(0)c(2\pi\nu H_M) = \frac{1}{\tilde{g}(0)}\left[\left(\frac{1}{\mu_i}\right)_\nu - \left(\frac{1}{\mu_i}\right)_0\right], \qquad (15)$$

where

$$\left(\frac{1}{\mu}\right)_\nu \stackrel{\text{def}}{=} \left(\frac{dH}{dB}\right)_{(0,0,2\pi\nu H_M)}.$$

In CMD5005, with the parameter values in Table 1, and the choice

$$\hat{g}(B) = \exp\left(\frac{-A_4|B|}{B_{cl} - |B|}\right),$$

a graph of μ_i *vs* ν yields the following

$$c(\dot{H}) = \begin{cases} 0, & \text{for } \dot{H} < 2 \times 10^7; \\ 3.1(\log(\dot{H}) - 7\log(2)), & \text{for } 2 \times 10^7 < \dot{H} < 9 \times 10^7; \\ 2.02 + 9.14(\log(\dot{H}) - 7\log(9)), & \text{for } 9 \times 10^7 < \dot{H} < 9 \times 10^8, \end{cases}$$

where the units of $\dot{H}$ are Oe/sec. Initial magnetization curves and major loops for CMD5005 are shown in Fig. 5 for a "dc" or slowly varying applied field, and in Fig. 6 for a field which ramps linearly between ± 12Oe at a rate of 96×10^6Oe/sec. These results are in good agreement with the manufacturer's dc hysteresis data and with experiments showing a loop shape similar to that in Fig. 6 and closure of the major loop around 12Oe for a sinusoidal field of approximately 2MHz.

Solutions of (13) were obtained by the same finite difference scheme (5) used for (4), with $\dot{H}$ held constant at each time step and the resulting values for $\hat{g}$ in (12) substituted for those of $\tilde{g}$.

ANISOTROPY IN THIN FILMS

Thin films used in magnetic recording exhibit an anisotropy that is approximately uniaxial with respect to the direction perpendicular to the surface of the film. Experimenters [7-8] report a dependence of hysteresis loop shapes and values on film preparation. Samples of major loops similar to those reported are shown in Figs. 7-9. The development of perpendicular recording has spurred an interest in vector hysteresis calculations, for which the representation of this anisotropy is fundamental.

I have attempted to lay the foundations for such a vector model by extending the theory described in (3)-(6) to the problem of representing in each direction the hysteretic behavior of a perfectly uniaxially anisotropic material. I shall assume that in each direction the material exhibits hysteretic behavior in accord with the rate independent theory. Representations for the perpendicular, $\psi = 0$, and the in-plane or parallel, $\psi = \pm\pi/2$, directions are obtained by evaluating the constants in (6) from hysteresis loops measured in those

directions. At the intermediate angles, I compute values for these constants, the closure field, and the permeability beyond closure by scaling between the extreme directions:

$$\begin{aligned} H_{cl}(\psi) &= H_{cl}(0) + h(\psi)[H_{cl}(\pi/2) - H_{cl}(0)], \\ \mu_{cl}(\psi) &= \mu_{cl}(0) + h(\psi)[\mu_{cl}(\pi/2) - \mu_{cl}(0)], \\ A_i(\psi) &= A_i(0) + h(\psi)[A_i(\pi/2) - A_i(0)], \end{aligned} \tag{16}$$

where $i = 1, 2, 3, 4$ and h is a scaling function of ψ with $h(0) = 0$ and $h(\pi/2) = 1$. There is currently no justification for (16) other than the agreement it produces between computations and experiments. For the CoCr films shown in Figs. 7-9, the scaling rule (16) with h a monotone increasing function of ψ yields hysteresis loops which change gradually with angle between the two extremes and are, at each direction, in accord with the principles of rate independent hysteresis. The choice,

$$h(\psi) = \begin{cases} 1 - \exp(-4\psi^2), & \text{for } |\psi| < \pi/2, \\ 1, & \text{for } |\psi| = \pi/2 \end{cases} \tag{17}$$

yields graphs of the angular variation of the coercive field that, in agreement with experiments, are bell-shaped for materials with fairly similar parallel and perpendicular behaviors, and M-shaped for preparations with rather dissimilar behaviors, as shown in Fig. 10.

In numerically simple and fast vector calculations based on these ideas, the previous state, $(H_0(\psi), B_0(\psi))$, in the direction of the vector magnetic field $\mathbf{H}$ is the projection of the vector state $(\mathbf{H}_0, \mathbf{B}_0)$ onto the ψ axis. The new state, (H, B), in the ψ direction is computed from (4)-(6) and (16). The flux density in the direction perpendicular to ψ is demagnetized as the magnitude of the resulting flux vector $\mathbf{B}$ exceeds a certain value, which I have taken to be the closure value, B_{cl}. A complete and more correct vector model awaits experimental clarification of the demagnetization process and of the effect on the ψ-directed magnetization of the perpendicular flux component. Both effects, in all likelihood, depend on ψ and its distance to the preferred axis of magnetization.

ACKNOWLEDGEMENTS

The author wishes to thank Dr. P. A. Arnold and Dr. B. E. Warner of Lawrence Livermore National Laboratory for their stimulating interest in this work and their generous support. The work was performed under the auspices of the U. S. Department of Energy.

REFERENCES

[1] B.D. Coleman, M.L. Hodgdon, "A Constitutive Relation for Rate Independent Hysteresis in Ferromagnetically Soft Materials," *Int. J. Engng. Sci.*, **24**, No. 6, 1986, pp. 897-919.

[2] B.D. Coleman, M.L. Hodgdon, "On a Class of Constitutive Relations for Ferromagnetic Hysteresis," to appear in *Arch. Rational Mech. Anal.*

[3] R. Bouc, "Modèle Mathématique d'hystérésis," *Acustica*, **24**, 1971, pp.16-25.

[4] R. M. Bozorth, *Ferromagnetism*, New York:Van Nostrand, pp.548-549.

[5] R. Becker, W. Döring, *Ferromagnetismus*, Berlin: Springer Verlog, 1939, pp. 242-252.

[6] S. Ball, Physics International, and E.G. Cook, Lawrence Livermore National Laboratory, private communications.

[7] J. S. Gau, C. F. Brucker, "Angular Variation of the Coercivity in Magnetic Recording Thin Films," *J. Appl. Phys.*, **57**, No. 1, 1985, pp. 3988-3990.

[8] R. Sugita, T. Kunieda, F. Kobayashi, "Co-Cr Prependicular Recording Medium by Vacuum Deposition," *IEEE Trans. Mag*, **MAG-17**, No. 17, 1981, pp. 3172-3174.

Table 1 Required hysteresis data and values for the material constants in eq. (6) for the ferromagnetic material Permalloy and the ferrites CMD5005 and C/7D. Units here are kGauss for flux densities and Oersteds for magnetic fields.

	PERMALLOY	CMD5005†	C/7D‡
B_{cl}	7. 58	2. 5	2. 5
H_{cl}	0. 12	5. 0	6. 6
B_r	6. 2	1. 8	1. 8
H_c	0. 03	0. 23	0. 35
μ_r	38. 66	0. 99	0. 897
μ_c	686. 245	6. 0	9. 0
μ_s	3. 1466	2.49×10^{-2}	1.887×10^{-2}
μ_{cl}	1. 5	1.0×10^{-3}	1.0×10^{-3}
α	1. 0	1. 0	1. 0
A_1	8.9929×10^{-3}	0. 3746	0. 4946
A_2	0. 19736	0. 5984	0. 598397
A_3	16. 724	−0. 76955	−0. 55789
A_4	0. 56187	3.7485×10^{-2}	1.22877×10^{-2}

†Ceramic Magnetics, Inc., Fairfield, NJ 07006
‡Stackpole Corp., St. Marys, PA 15857

Table 2 Some hysteresis data and values for the material constants in eq. (6) for the sample preparations of CoCr thin film shown in Figs. 7-9. Here, flux densities are given in units of kGauss, and values for the magnetic fields are in kOersteds.

	$CoCr(\psi = \pm 90°)$	$CoCr(\psi = 0)^1$	$CoCr(\psi = 0)^2$
B_{cl}	7. 0	7. 0	7. 0
H_{cl}	4. 0	5. 4	7. 0
H_c	0. 6	1. 32	0. 9
μ_{cl}	0. 013	0. 185	0. 0275
α	1. 0	1. 0	1. 0
A_1	0. 8459	2. 759	5. 676
A_2	0. 1946	0. 1675	0. 1271
A_3	−3. 859	−2. 885	−1. 7074
A_4	0. 5889	0. 3254	0. 1147

Fig. 1 Initial magnetization curve and major loops for a Mn-Zn ferrite computed by numerical integration of eq. (1). Here, $\alpha = 1$, $f(H) = 5000 \tan 1.3H + \mu_0 H$, and $g(H) = f'(H)[1 - 0.58\exp(-2.3|H|)]$.

Fig. 2 Initial magnetization curve for Permalloy from eqs. (5-6). Flux densities and fields at the labled points (H_{cl}, B_{cl}), $(H_s, 0)$, and $(0, B_r)$, and the slopes μ_{cl}, μ_s, μ_c, and μ_r are used in calculating the values given in Table 1 for the constants in eqs. (6).

Fig. 3 Material functions $\tilde{f}$ (solid curve) and $\tilde{g}$ (dashed curve) from the Permalloy values in Table 1. (**Fig. 4** Solutions curves of eq. (4) showing convergence in Permalloy from full magnetic remanence, $(0, B_r)$, to the minor loop associated with oscillations of H between ± 50mOe. A discussion of convergence to such loops and their stability is given in [1] and [2].

Fig. 5 Initial magnetization curve and major loop for CMD5005 from eqs. (5-6). Values of the material constants in (6) are given in Table 1.

Fig. 6 Initial magnetization curve and major loop for CMD5005 from eqs. (13-15) for an applied field ramping linearly between ± 12Oe at the rate of 96×10^6Oe/sec.

Fig. 7 Initial magnetization curve and major loop for the parallel or in-plane axis of a CoCr film from eqs (5-6). Values for the material constants in (6) are given in the first column in Table 2.

Fig. 8 Initial magnetization curve and major loop for the perpendicular direction in a CoCr film from eqs. (5-6) for the values given in the second column in Table 2.

Fig. 9 Initial magnetization curve and major loop for the perpendicular direction in a CoCr film from eqs. (5-6) for the values given in the third column in Table 2.

Fig. 10 Angular variations in the coercivity for two preparations of CoCr film. The bell-shaped curve (solid) corresponds to a film in which the major hysteresis loops are as shown in Figs. 7-8. The M-shaped curve (dashed) corresponds to one in which the hysteresis loops are in Figs. 7 and 9.

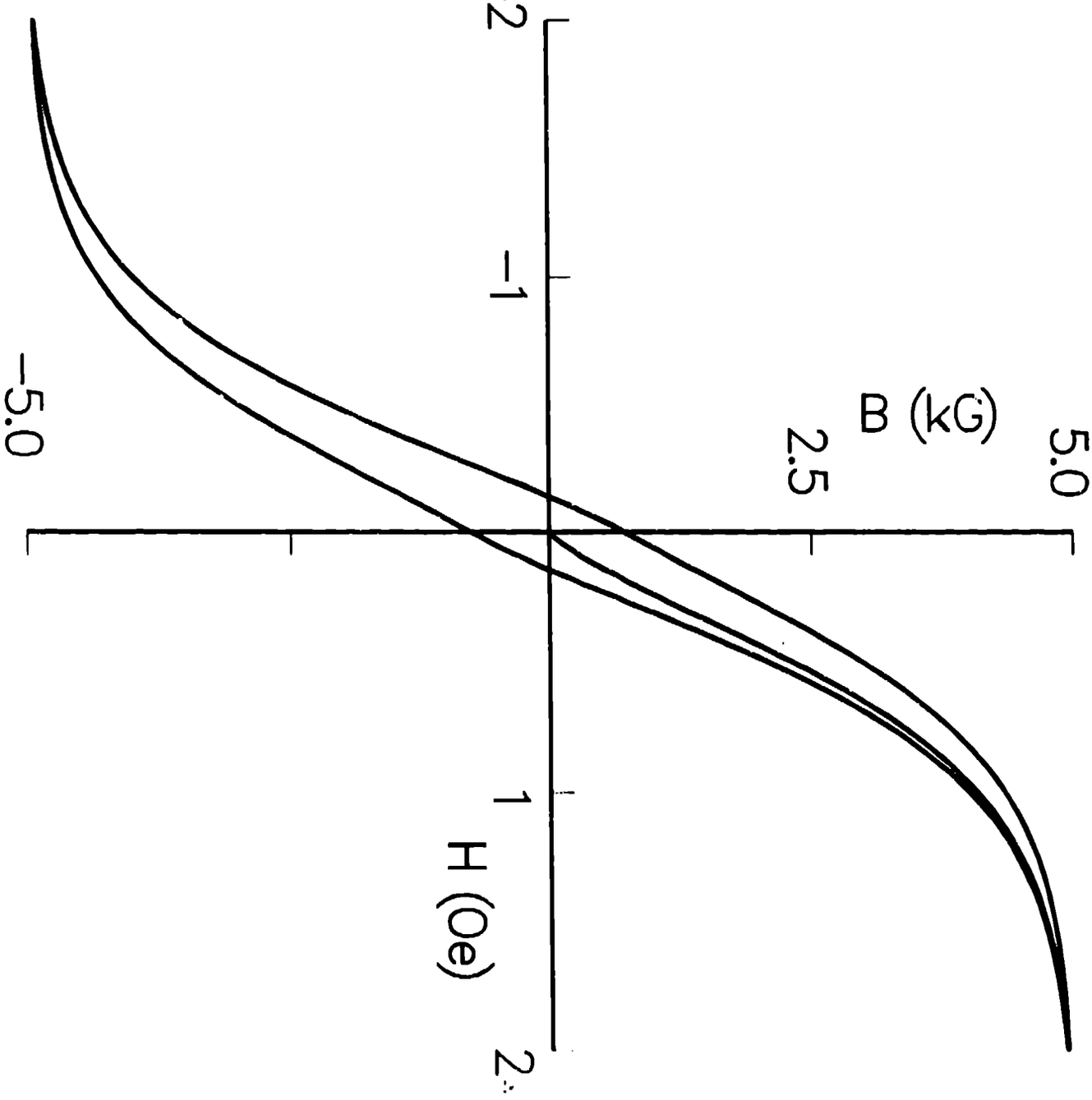
−2
−1
−5.0
B (kG)
2.5
5.0
1
H (Oe)
2

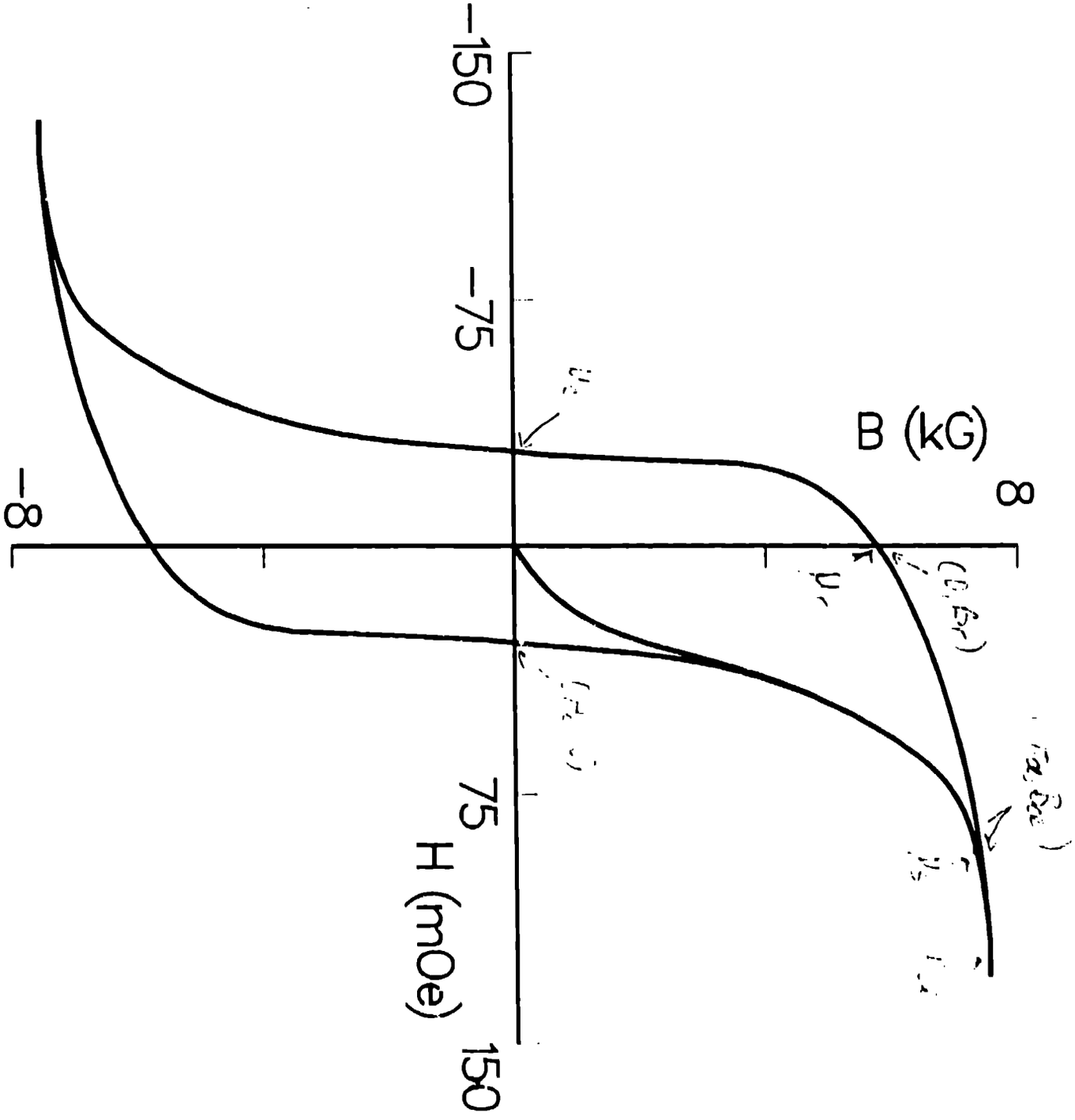
−150
−75
B (kG)
−8
8
75
H (mOe)
150

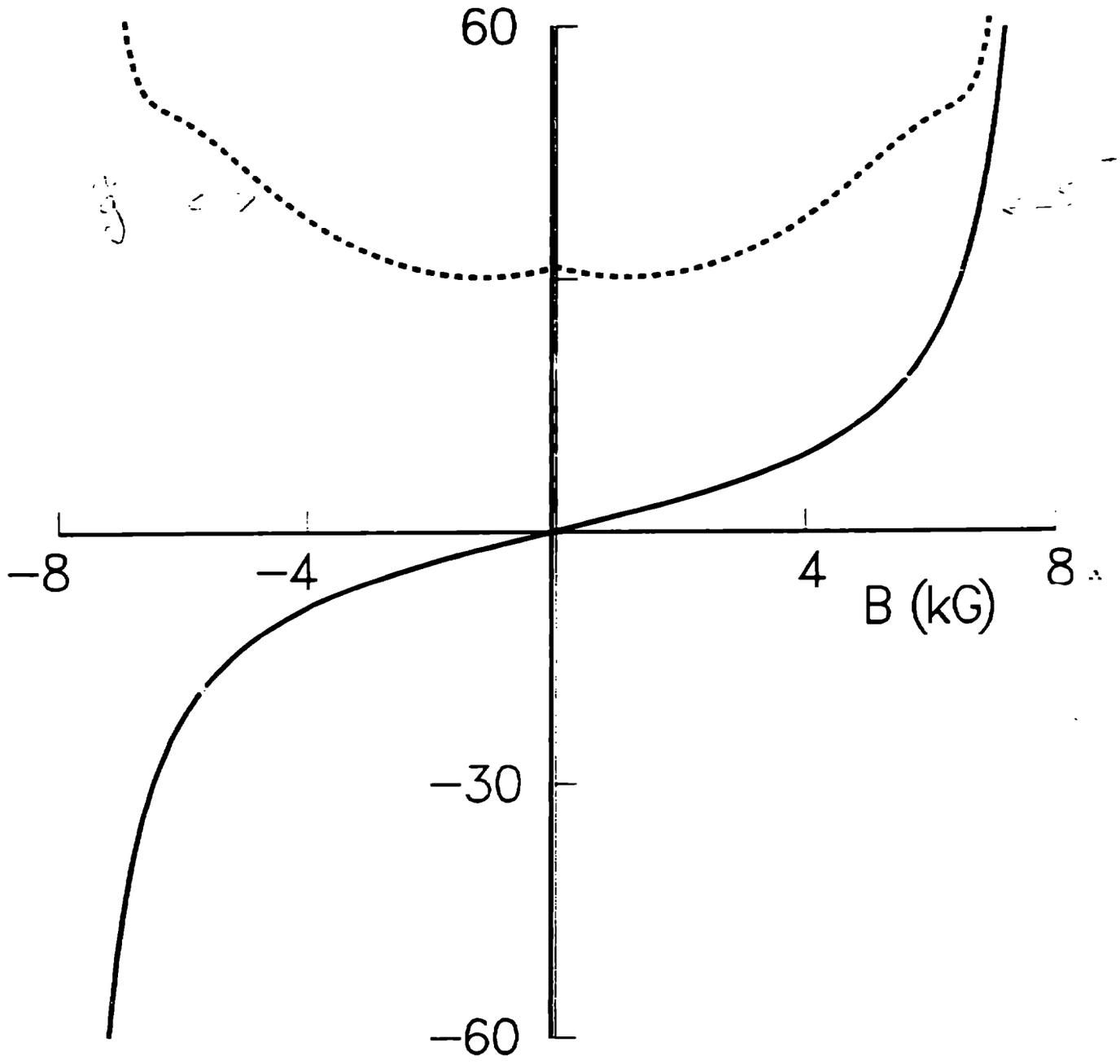

9

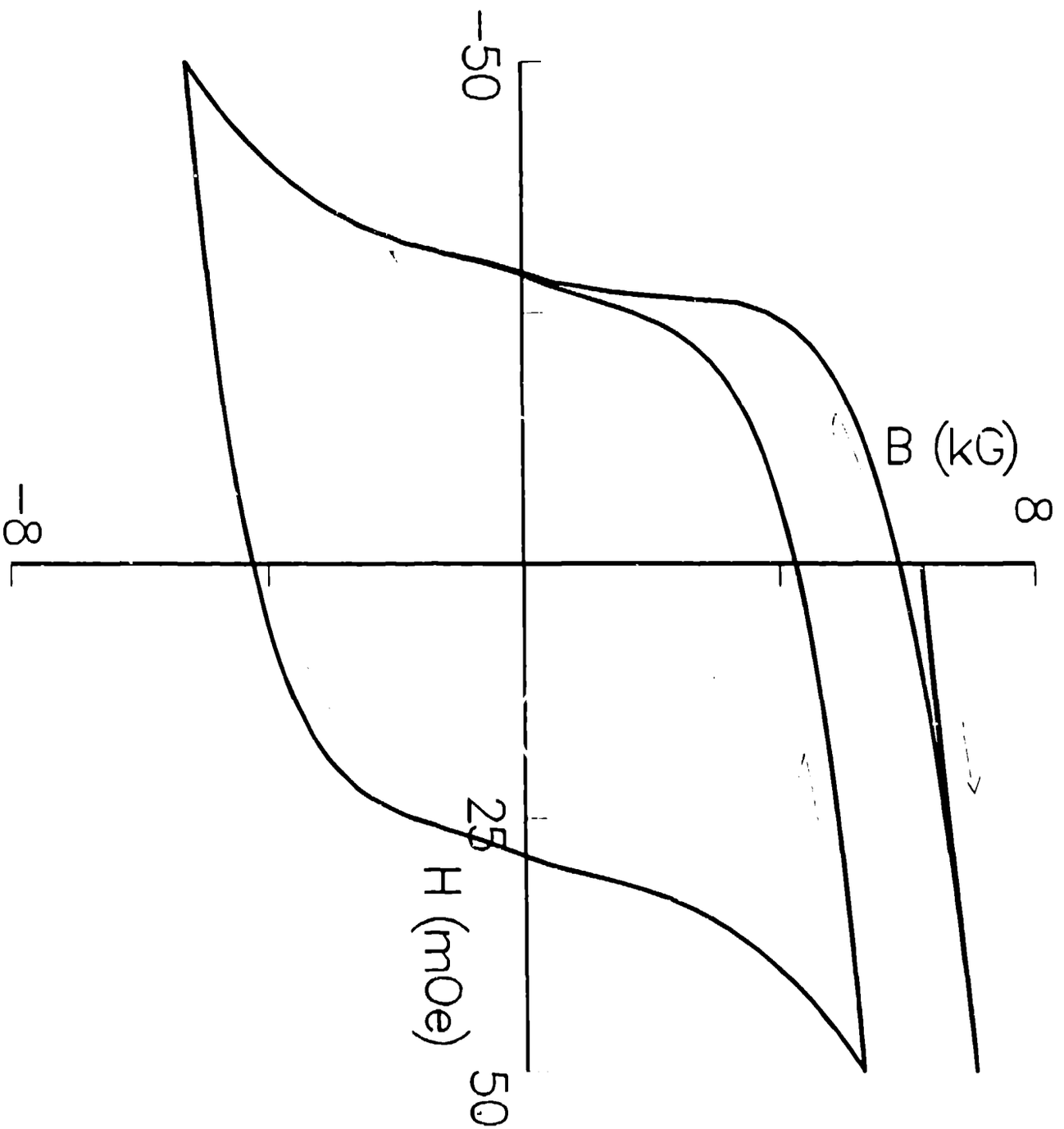
-50
B (kG)
-∞
∞
25
H (mOe)
50

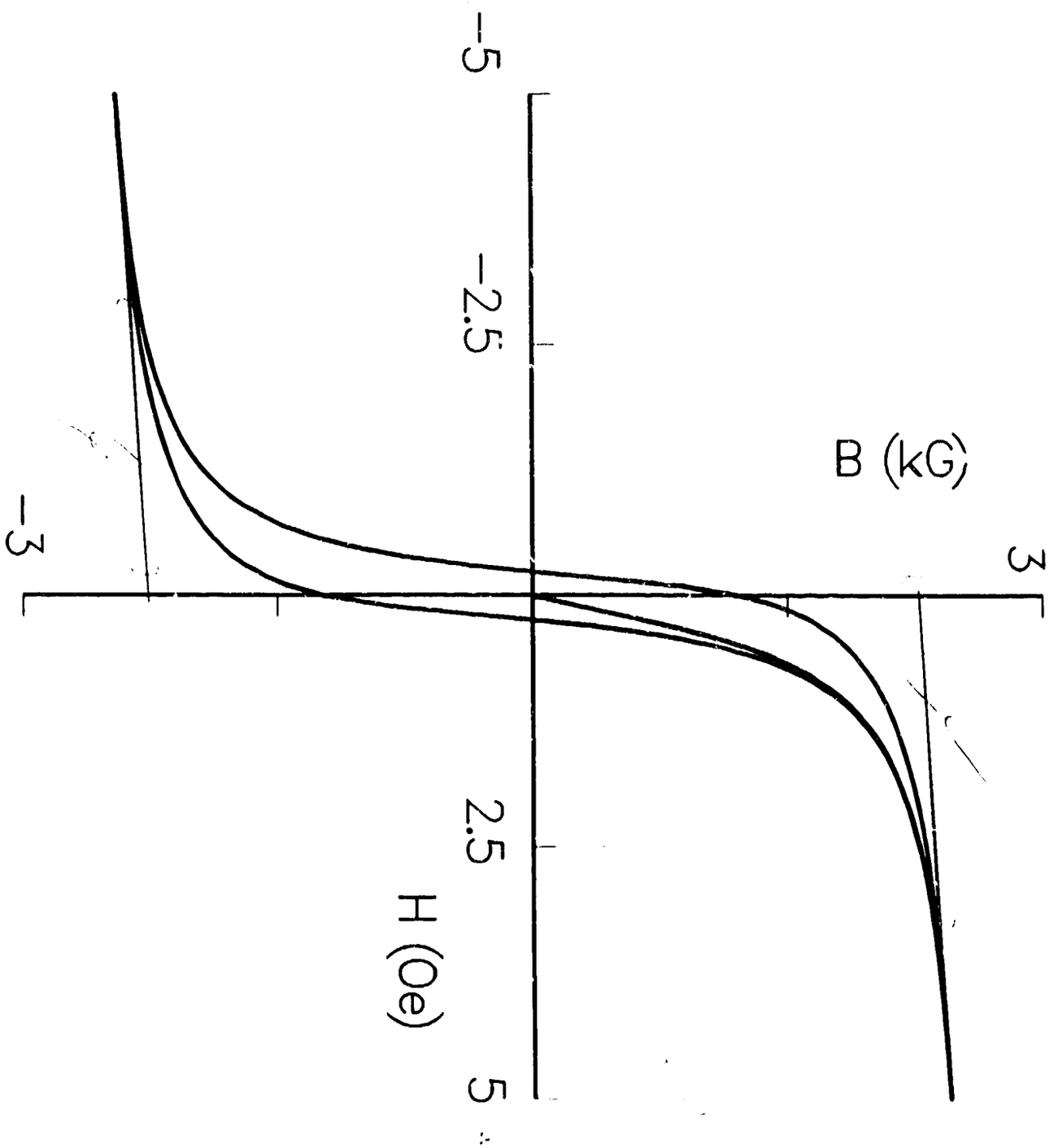
-5
-2.5
B (kG)
-3
3
2.5
H (Oe)
5

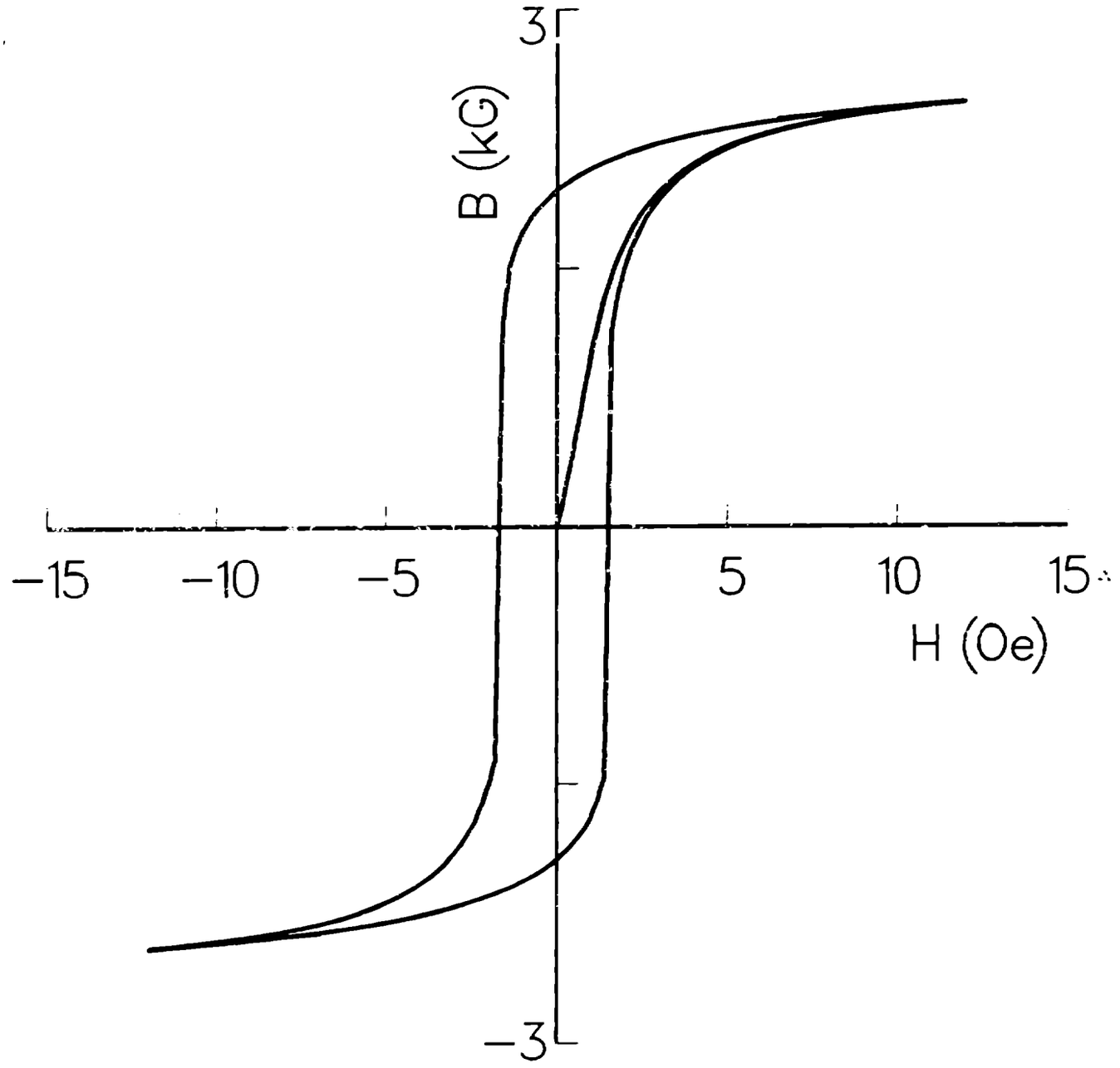

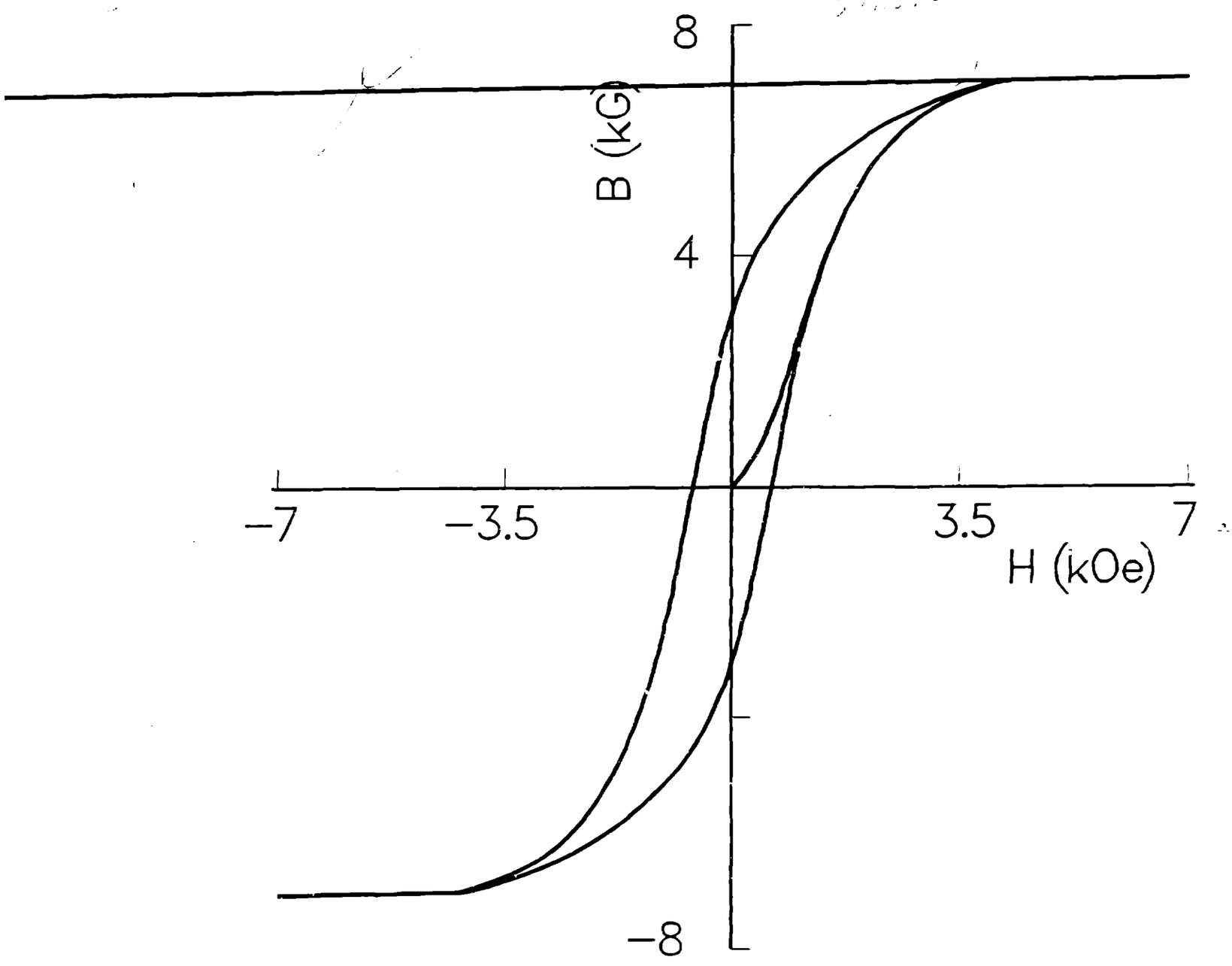
8
4
−8
B (kG)
−7
−3.5
3.5
7
H (kOe)

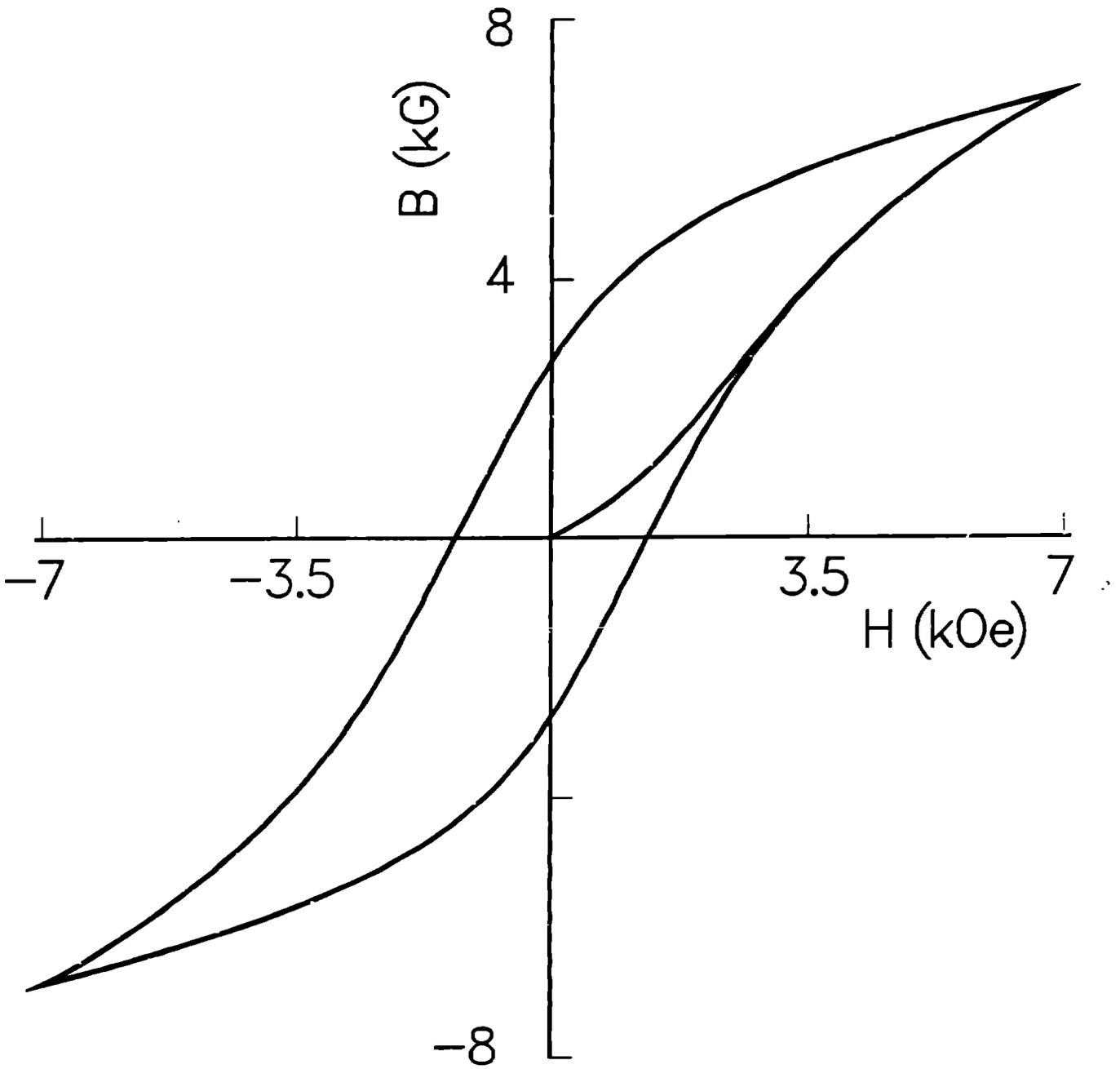
8
B (kG)
4
−7
−3.5
3.5
7
H (kOe)
−8

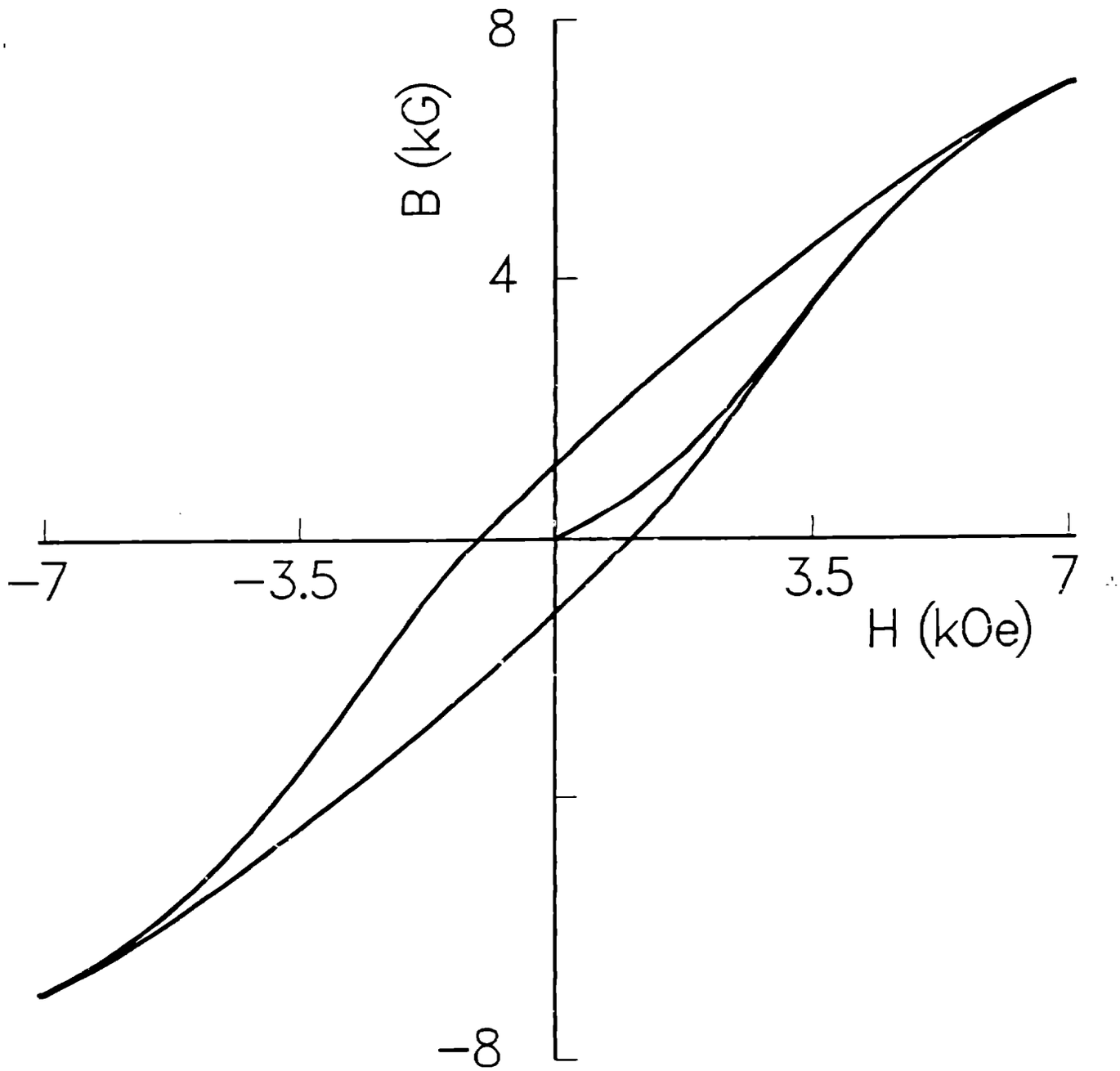
8
B (kG)
4
−7
−3.5
3.5
7
H (kOe)
−8

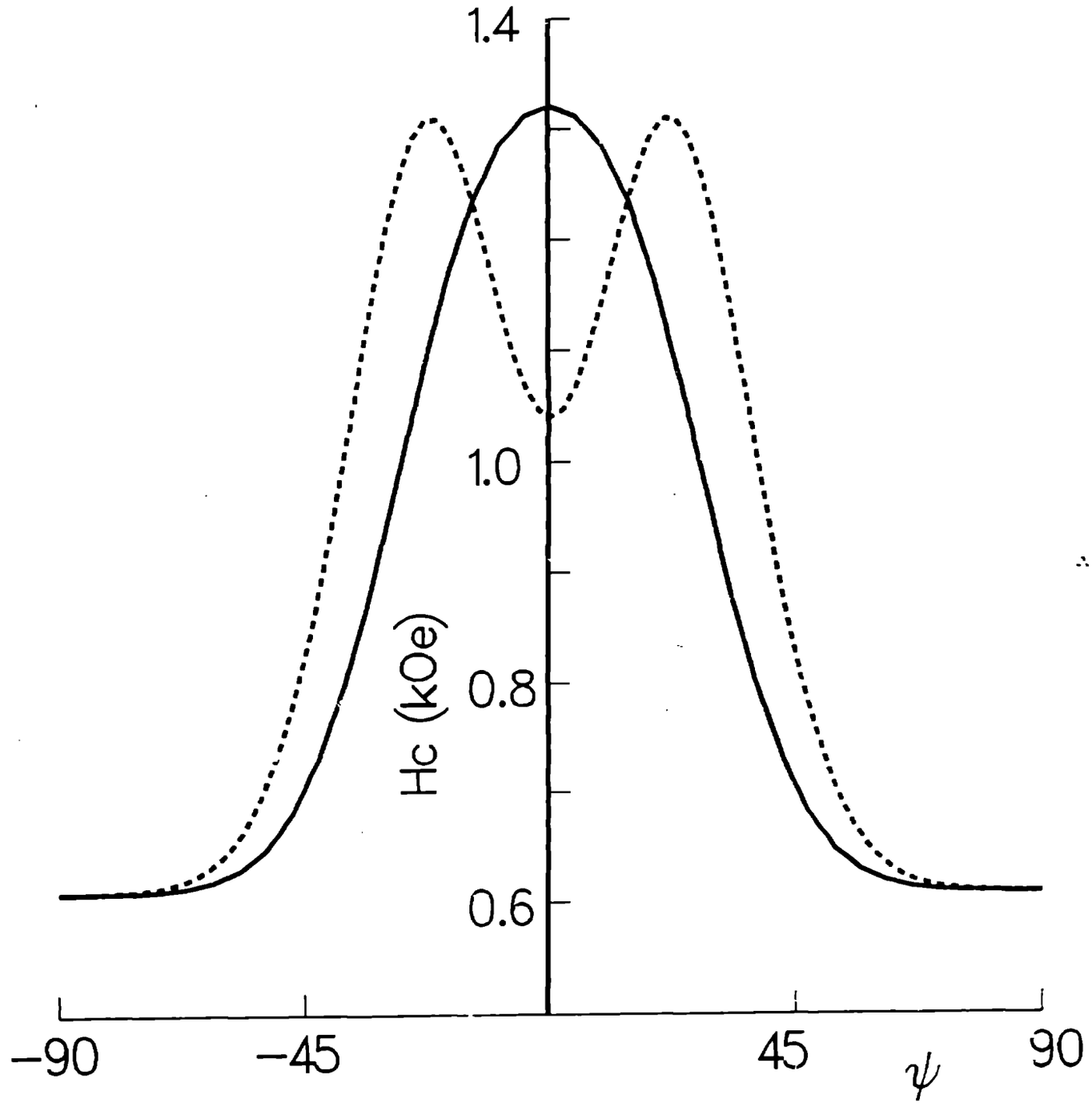
1.4
1.0
0.8
0.6
Hc (kOe)
−90
−45
45
90
ψ